

# Sustainable production of nanoemulsions by membrane-assisted nanoemulsification using novel aroma-based hydrophobic deep eutectic solvents for enhanced antifungal activities

S. Mondal<sup>a</sup>, U.T. Syed<sup>a,\*,\*\*</sup>, E. Pinto<sup>b,c</sup>, I.C. Leonardo<sup>d,e</sup>, P. Romero<sup>f</sup>, F.B. Gaspar<sup>d,e</sup>, M.T. Barreto Crespo<sup>d,e</sup>, V. Sebastian<sup>g,h,i</sup>, J.G. Crespo<sup>a,e</sup>, C. Brazinha<sup>a,\*</sup>

<sup>a</sup> LAQV/Requimte, Department of Chemistry, NOVA School of Science and Technology, FCT NOVA, Universidade NOVA de Lisboa, 2829-516, Caparica, Portugal

<sup>b</sup> CIIMAR - Interdisciplinary Centre of Marine and Environmental Research, Terminal de Cruzeiros do Porto de Leixões, 4450-208, Matosinhos, Portugal

<sup>c</sup> Laboratory of Microbiology, Department of Biological Sciences, Faculty of Pharmacy, University of Porto, Rua de Jorge Viterbo Ferreira, 228, 4050-313, Porto, Portugal

<sup>d</sup> Food & Health Division, iBET, Instituto de Biologia Experimental e Tecnológica, Apartado 12, 2781-901, Oeiras, Portugal

<sup>e</sup> ITQB-NOVA, Instituto de Tecnologia Química e Biológica António Xavier, Universidade NOVA de Lisboa, Av. da República, 2780-157, Oeiras, Portugal

<sup>f</sup> Department of Organic Chemistry, Instituto de Nanociencia y Materiales de Aragón (INMA), CSIC-Universidad de Zaragoza, Zaragoza, Spain

<sup>g</sup> Department of Chemical Engineering, University of Zaragoza, Campus Río Ebro-Edificio I+D, C/ Poeta Mariano Esquillor S/N, 50018, Zaragoza, Spain

<sup>h</sup> Instituto de Nanociencia y Materiales de Aragón (INMA), CSIC-Universidad de Zaragoza, Zaragoza, 50009, Spain

<sup>i</sup> Networking Research Center on Bioengineering, Biomaterials and Nanomedicine, CIBER-BBN, 28029, Madrid, Spain

## ARTICLE INFO

Handling Editor: Kathleen Aviso

### Keywords:

Hydrophobic deep eutectic solvent  
Nanoemulsions  
Delivery systems  
Natural compounds  
Antimicrobial properties  
NMR analysis

## ABSTRACT

Hydrophobic deep eutectic solvents (DESs), a recent class of green solvents, offer 100% atom economy, low cost, potential biodegradability, negligible toxicity and promising bioactivities. In this work, novel aroma-based therapeutic hydrophobic DESs were prepared and dispersed in aqueous media as nanoemulsions to potentiate biomedical applications, where polar media is encountered.

A reusable microengineered stainless-steel isoporous membrane was fabricated by laser drilling technique. Three hydrophobic DESs, namely DES A (menthol and vanillin), DES B (menthol and raspberry ketone), and DES C (thymol and raspberry ketone) were prepared and emulsified in aqueous media by sustainable membrane emulsification technique. The optimised nanoemulsion (DES C-in-water) exhibited a monomodal size distribution with  $Z_{avg}$  (size average) of 147 nm and polydispersity index of 0.22.

From the application perspective, the formulated DES-in-water nanoemulsions and their constituents were evaluated for their antibacterial properties against *Escherichia coli* and *Staphylococcus aureus*. Additionally, antifungal properties of the DES-based emulsions were reported for the first time by testing them against four fungal strains, *Aspergillus fumigatus*, *Candida albicans*, *Candida krusei*, and *Trichophyton mentagrophytes*. The nanoemulsions were found to exhibit antimicrobial effect and lesser quantities of individual compounds were needed in nanoemulsified state to show similar effects. Different 1D and 2D NMR techniques were successfully used to investigate the structural orientation and the inter and intramolecular interactions in the DES and emulsion systems, which revealed a probable cause for higher antimicrobial activity of DES C-based emulsions compared to its peers. Lastly, a synergistic effect of the components in nanoemulsions led to enhanced antimicrobial activities.

## 1. Introduction

Antibiotic resistance is one of the appalling mongers in the global health ecosystem. A growing number of infections are becoming more difficult or impossible to treat due to the inefficiency of available

antibiotics (Larsson and Flach, 2022). Also, food industries seek the possibility of finding new antimicrobials that can be used in the production (good hygiene practices) and processing of foods. The quest for novel pharmacologically active agents resulted in the discovery of many clinically useful drugs (e.g., bacteriocins) that play a key role in fighting

\* Corresponding author.

\*\* Corresponding author.

E-mail addresses: [s.taqui@campus.fct.unl.pt](mailto:s.taqui@campus.fct.unl.pt) (U.T. Syed), [c.brazinha@fct.unl.pt](mailto:c.brazinha@fct.unl.pt) (C. Brazinha).

<https://doi.org/10.1016/j.jclepro.2024.141167>

Received 16 August 2023; Received in revised form 1 January 2024; Accepted 6 February 2024

Available online 12 February 2024

0959-6526/© 2024 The Authors. Published by Elsevier Ltd. This is an open access article under the CC BY license (<http://creativecommons.org/licenses/by/4.0/>).

diseases of microbial origin (Hassan et al., 2012). However, various side effects of these antimicrobial agents led food and pharmaceutical industries to seek natural product-based alternatives (because of their innate tolerance in the human body) (Miethke et al., 2021).

Components of natural essential oils such as thymol and menthol and some food-grade aromas qualify as potential alternatives. Extensive research has indicated that thymol acts as an antimicrobial agent by depolarization and further damaging bacterial cell membranes but a high concentration of thymol is necessary for the therapeutic purpose (Bergua et al., 2021). Thymol exhibited antifungal activity at lower concentrations and the activity mechanism was found to also involve depolarization of the cytoplasmic membrane (Vale-Silva Maria José; Cavaleiro, Carlos; Salgueiro, Lígia; Pinto, Eugénia, 2010). Moreover, compounds exhibiting high melting points, low water solubilities, and/or high costs represent a challenge when used as a preservative (Schultheiss and Newman, 2009).

In the last decades, along with the world trend for sustainability, there is a need to develop green solvents to mitigate toxicity caused by traditional organic solvents. In 2001, Abbot et al. introduced deep eutectic solvents (DES) which are defined as a mixture of two or more solid compounds with high melting points which, when mixed at fixed molar ratios, lead to the formation of a liquid phase with significant lower melting point. The dip in the melting point is mainly caused by charge delocalization from hydrogen bond formation (Smith et al., 2014). Some other promising advantages of such DESs are facile preparation by low-cost methods, 100% atom economy (their preparation does not originate any by-products), biodegradability, and tunability (Cao and Su, 2021; Mondal et al., 2023; Zhang et al., 2023). Even without the existence of standardized methods adapted to testing the antimicrobial activities of DESs, to ensure a straightforward comparison between the results obtained, numerous studies undeniably demonstrate their ability to inhibit the growth of microorganisms, either bacteria, yeasts, or moulds (Marchel et al., 2022; Rodríguez-Juan et al., 2021; Syed et al., 2020). Interestingly, hydrophobic DESs have been recently reported in the domain of green chemistry (D. Ribeiro et al., 2015; van Osch et al., 2015). This phenomenon of mixing two or more solid hydrophobic compounds to form a homogeneous liquid phase provides additional competitive advantages such as high solubility of water-insoluble drugs and enhanced therapeutic value by the synergistic effect, to mention a few (Van Osch et al., 2020). Apart from biomedical applications, some other notable applications are selective volatile organic compounds removal, green extraction of various organic compounds, removal of pollutants from wastewater (Makoś et al., 2018; Marchel et al., 2023; Momotko et al., 2022). The utility of hydrophobic DESs for bio-based applications is limited as they exhibit low or negligible water solubility. In most antimicrobial agents for food and biomedical applications, polar-based media are required, and hence a prudent solution is to extract the boons of therapeutic DESs by dispersing them into an emulsion system, particularly through oil-in-water (O/W) emulsions (Syed et al., 2020). Emulsions of therapeutic oils are colloidal systems that exhibit enhanced bioactivities and minimise adverse organoleptic effects (Prakash et al., 2018). Also, research confirms the advantages of a nano-sized emulsion in comparison to its peers because of improved antimicrobial activity due to the high specific area of nanometric droplets and greater kinetic stability (Chuacharoen and Sabliov, 2019; He et al., 2022).

Nanoemulsions are conventionally formed using high energy-intensive methods like high-pressure homogenisation and ultrasonication (Gupta, 2020). However, the use of direct membrane emulsification is a more sustainable approach as it saves energy by 2 orders of magnitude without compromising the emulsion quality (Usman Taqui Syed et al., 2022). In this process, the dispersed phase is pressurised through the membrane pores and dispersed into the circulating continuous phase. The droplet size and size distribution mostly depend on the membrane pore size, membrane material, pore geometry, physical characteristics of both phases, and their flow conditions (Güell et al.,

2016; Piacentini et al., 2014a). Polymeric membranes, Shirasu porous glass (SPG) membranes, and anodic alumina membranes are generally used in direct membrane emulsification processes (Lee and Mattia, 2013; Mondal et al., 2022; Piacentini et al., 2014b). However, those membranes possess disadvantages for membrane emulsification processes, such as uneven pore size and distribution, thickness and high tortuosity that culminates into hindrance for the formation of narrow size distributed nanoemulsions. Also, the literature suggests that homogenizers and sonicators depend on the concentration and composition of suitable surfactants to produce stable nanoemulsions (Syed et al., 2021). On the other hand, direct membrane emulsification is a cost-effective technique as it does not depend on expensive surfactant(s). Lower quantities of surfactants are sufficient enough in direct membrane emulsification wherein the bulk of the droplet breakdown is achieved due to the pore sizes of the membranes (Syed et al., 2022). However, the size of the emulsion droplets is typically 2–10 times the size of the membrane pores (Charcosset et al., 2004).

Considering the scientific challenges mentioned above, this work was devoted to sustainably formulating novel hydrophobic DESs (using products of natural origin) and DESs-based nanoemulsion systems and exploring their antimicrobial activity. Although few studies have reported the potentialities of hydrophobic DES-based emulsions as antibacterial agents, the exploration of their antifungal properties was, to our knowledge, not yet reported, and it sets the premise of the present study (Syed et al., 2020). Also, advanced NMR techniques were used to further elucidate the mechanism of the observed antimicrobial behaviour.

## 2. Materials and methods

### 2.1. Materials

Menthol, thymol, vanillin, and raspberry ketone ( $\geq 98\%$ ,  $\geq 98.5\%$ ,  $99\%$ , and  $\geq 98\%$  purity, respectively, Sigma Aldrich, Germany) were used to prepare novel hydrophobic DESs with diverse molar compositions. Hydrophobic DESs, comprising these components with selected molar ratios, were pumped through specifically fabricated membranes into an aqueous phase containing Tween 80 (Sigma Aldrich, Germany) in Milli-Q water. These two phases were, respectively, the dispersed and the continuous phases to formulate DES-in-water nanoemulsions. Laser-drilled microengineered membranes made of AISI 304 stainless steel foils (Record Metall-Folien GmbH Company, Germany) were fabricated as previously reported by Syed et al. (2020). The selected DESs, their components, and the optimised nanoemulsions were tested for their antibacterial activities against *S. aureus* ATCC 6538 and *E. coli* ATCC 8739 bacterial strains. Also, the same samples were tested for their antifungal activities against *C. albicans* ATCC 10231, *C. krusei* ATCC 6258, *A. fumigatus* ATCC 204305, and *T. mentagrophytes* FF7 fungal strains.

### 2.2. Preparation and characterisation of therapeutic hydrophobic deep eutectic solvents (DESs)

#### 2.2.1. Preparation of hydrophobic DESs

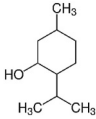
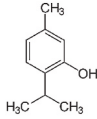
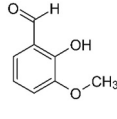
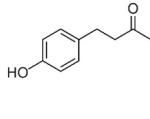
Combinations of a monoterpene, like menthol and thymol, with aroma compounds, like vanillin and raspberry ketones, were combined at different molar compositions in attempt to prepare DES (ranging from molar ratios of 1:9 until 9:1, following the protocol described in works of Syed et al. (Syed et al., 2020; Usman T Syed et al., 2022)). Table 1 depicts the physicochemical properties of the hydrophobic components used in attempting to prepare the DESs.

#### 2.2.2. Characterisation of hydrophobic DESs

All the successfully prepared hydrophobic DESs were subjected to Karl-Fischer titration (KF Coulometer, Metrohm) to measure their water content. Prior to the emulsification studies, the phase transition

**Table 1**

Physicochemical properties of the constituents of DESs.

	Menthol	Thymol	Vanillin	Raspberry ketone
Chemical formula	C <sub>10</sub> H <sub>20</sub> O	C <sub>10</sub> H <sub>14</sub> O	C <sub>8</sub> H <sub>8</sub> O <sub>3</sub>	C <sub>10</sub> H <sub>12</sub> O <sub>2</sub>
Molar mass (g.mol <sup>-1</sup> )	156.27	150.22	152.15	164.20
Melting point (°C)	34–36	48–51	81–83	82–84
Density (g.ml <sup>-1</sup> at 25 °C)	0.890	0.965	1.056	1.033
Solubility in water (g.l <sup>-1</sup> at 25 °C)	0.42	0.90	10.00	Data not available
Hydrogen bond donor sites	1	1	1	1
Hydrogen bond acceptor sites	1	1	3	2
Chemical structure				

behaviour of the selected eutectic mixtures with higher quantities of terpene-based bioactive compounds was evaluated by differential scanning calorimetry (DSC) (TA Instruments Q-series TM Q2000 DSC). The refractive indices were determined by a refractometer (ABBEMAT 500, Anton Paar, Austria). The density and viscosity measurements of these selected DESs were also carried out using an automatic kinematic viscometer (Automated SVM 3000, Anton Paar, Austria) (see Section S1 of the supplementary material for further experimental details).

### 2.3. Formulation of DES-in-water nanoemulsions

#### 2.3.1. Membrane emulsification experiments

DES-in-water nanoemulsions were formulated using the membrane emulsification set-up, a schematic representation of which is illustrated in Fig. 1 (see Section S2 of the supplementary material for details of the membrane and its fabrication). Different volumetric concentrations of 2%, 4%, and 6% (v/v) of the dispersed phase into the continuous phase were tested to produce emulsions (50 ml volume). For a comparative analysis of the therapeutic efficacy of the produced DES-in-water nanoemulsions with works of Syed et al., 2% (v/v) of Tween 80 surfactant dissolved in the aqueous phase was kept constant throughout the study (Syed et al., 2020, 2022). The dispersed phase was injected into the continuous phase, operating in crossflow mode, of the membrane emulsification unit by using a syringe pump (Harvard Apparatus, PHD ULTRA 4400 I/W PROG, USA) at different flow rates, namely 0.1 ml min<sup>-1</sup> and 0.05 ml min<sup>-1</sup>. A peristaltic pump (Velp Scientific, SP311, Italy) was used to recirculate the continuous phase flowing tangentially over the membrane surface. Since a higher continuous phase crossflow velocity facilitates droplet detachment from the membrane surface, the recirculation rate was fixed at 150 ml min<sup>-1</sup>, which was the highest possible pump velocity. The continuous phase crossflow velocity  $\nu_c$  [m.

s<sup>-1</sup>] was calculated as follows:

$$\nu_c = \frac{4 * Q_{CP}}{\pi * d_h^2} \quad (\text{Eq. 1})$$

where symbols  $Q_{CP}$  [m<sup>3</sup>.s<sup>-1</sup>] and  $d_h$  [m] denotes the continuous phase flow rate and the hydraulic diameter of the flow channel of the continuous phase in the membrane module respectively. Also,  $d_h$  depends on  $A$  [m<sup>2</sup>], the cross-sectional area of the channel and  $P$  [m] the wet perimeter of the channel as follows:

$$d_h = \frac{4A}{P} \quad (\text{Eq. 2})$$

A microengineered laser-drilled stainless steel reusable membrane having a uniform pore size of 9 μm and pore pitch (distance between two pores) of 100 μm was fabricated. Figs. S1 and S2 in the supplementary material depict the schematic representation of the laser drilling equipment and the surface analysis of the membrane, respectively.

#### 2.3.2. Characterisation of the produced DES-in-water nanoemulsions

A particle size analyser (Malvern Instruments, Nano ZS 90, UK) was used to measure the droplet sizes and size distributions by principles of dynamic light scattering (DLS). Furthermore, these results were confirmed by carrying out microscopy studies with a Transmission Electron Microscope (TEM Tecnai T20, FEI company, USA). The experimental details of the characterisation techniques are mentioned in Section S3 of the supplementary material.

#### 2.4. Characterisation of the two phases and of the membrane used to produce DES-in-water nanoemulsions

A drop shape analyser (DSA 25B, Krüss GmbH, Germany) was used to

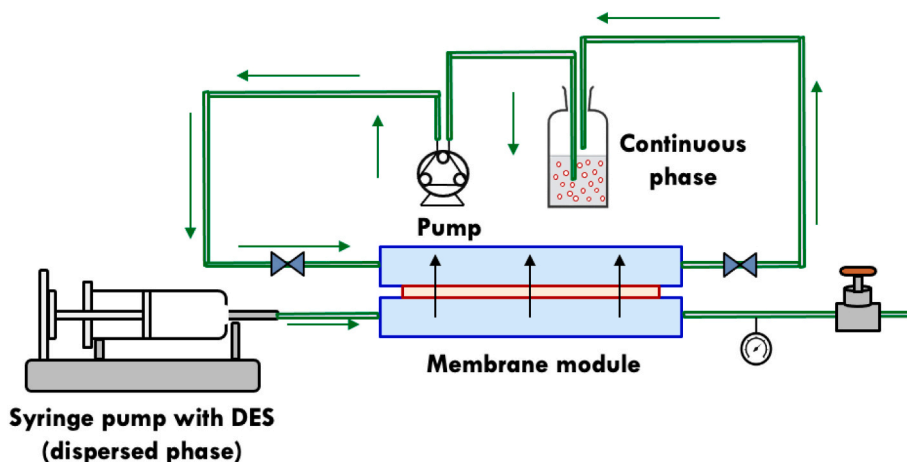


**Fig. 1.** Schematic representation of the membrane emulsification unit used for the sustainable production of DES-in-water nanoemulsions.

measure the interfacial tension between the aqueous phase and dispersed phases. It was also used to determine the hydrophilicity/hydrophobicity of the membrane surface by measuring the static water contact angle, and the contact angle of selected hydrophobic DESs on the membrane surface (see Section S4 of the supplementary material for further experimental details).

## 2.5. Antimicrobial susceptibility testing of the optimised DES-in-water nanoemulsions and their components

The antimicrobial activities were evaluated by determining the sample's minimum inhibitory concentration (MIC), minimum bactericidal concentration (MBC), and minimum fungicidal concentration (MFC). MIC values were the lowest concentration of an antimicrobial agent required to inhibit the visible growth after incubation. MBC values were the lowest concentration of the agents required to reduce at least 99.9% of bacterial viable counts, when compared to the initial inoculum and for the same incubation time. MFC values corresponded to the lowest concentration of antimicrobial agent at which 99.9% of the fungal inoculum dies. Results were expressed as a median of the MIC, MBC, and MFC values obtained in each of at least three biological replicates.

### 2.5.1. Antibacterial studies

The antimicrobial susceptibility testing (AST) assays were performed according to the broth microdilution method following the Clinical and Laboratory Standard Institute (CLSI M07-A10) guidelines (W.PA, 2015). Due to the white and opaque nature of the emulsions, the MIC value reading was performed using the cell viability reagent PrestoBlue™ (Invitrogen, San Diego, CA USA) according to the manufacturer's instructions (see Section S5 of supplementary material for further experimental details).

### 2.5.2. Antifungal studies

The broth microdilution method, based on the CLSI reference documents M27-A3 and M38-A2, was used to determine MIC for yeasts and filamentous fungi, respectively (PA, 2002; W.PA, 2008). Owing to the white and opaque nature of the emulsions, the MIC value reading was confirmed by microscopic analysis (see Section S5 of supplementary material for further experimental details).

## 2.6. Structural analysis of DES and DES-in-water nanoemulsion using nuclear Magnetic Resonance (NMR)

NMR experiments were performed with a Bruker AVANCE 500 spectrometer operating at a frequency of 500.13 MHz for  $^1\text{H}$  and 125.75 MHz for  $^{13}\text{C}$  using standard pulse sequences. For DESs, the spectra were recorded in neat eutectic and capillary inserts with  $\text{D}_2\text{O}$  and TMSP- $\text{d}_4$  (3-(Trimethylsilyl)propionic-2,2,3,3- $\text{d}_4$  acid sodium salt) were used for lock and internal reference. The unequivocal assignment of the signals was verified using 2D  $^1\text{H}$ - $^1\text{H}$  DQF-COSY (Correlated Spectroscopy),  $^1\text{H}$ - $^{13}\text{C}$  HSQC (Heteronuclear Single Quantum Coherence) and  $^1\text{H}$ - $^{13}\text{C}$  HMBC (Heteronuclear multiple-bond Coherence) experiments.

In order to determine the structural orientation of the components of DESs and the DESs-in-water nanoemulsions NMR experiments based on the Nuclear Overhauser (NOESY and ROESY) were carried out. Thus,  $^1\text{H}$ - $^1\text{H}$  NOESY (Nuclear Overhauser Effect Spectroscopy) spectra were recorded with mixing times of 50, 200, 400, 800 and 1000 ms each with gradient pulses applied during mixing time.  $^1\text{H}$ - $^1\text{H}$  ROESY (Rotating-frame Overhauser Effect Spectroscopy) experiments were recorded at mixing time of 400 ms.

Pulsed Field Gradient (PFG) NMR was used to perform  $^1\text{H}$  DOSY (Diffusion ordered Spectroscopy) spectra using a stimulated echo sequence with bipolar sine gradient pulses and eddy current delay before the detection (BPLED). Diffusion time ( $\Delta$ ) was set within the interval 200–300 ms. The pulsed gradients were incremented from 2 to

95% of the maximum strength in 16 or 32 spaced steps with a duration ( $\delta$ ) of 2–4 ms. In these spectra, the attenuation of the NMR signal can be related to the diffusion coefficient (Stejskal-Tanner equation) (see section S6 of supplementary materials for further details).

## 3. Results and discussions

### 3.1. Preparation and characterisation of aroma compounds-based therapeutic hydrophobic DESs

In the pursuit of obtaining therapeutic DES-in-water nanoemulsions targeted for biomedical applications, where typically aqueous media are required, the current study aims to explore hydrophobic aroma compounds such as vanillin and raspberry ketones for the preparation of novel DESs. These aroma compounds are also reported to have certain therapeutic value (Hamdy et al., 2022; Peña-Gómez et al., 2019). As a second hydrophobic compound that can act as a hydrogen bond donor/acceptor in combination with these aroma compounds, menthol, and thymol commonly utilised as therapeutic terpenes, were explored. These non-ionic terpenes are widely reported for their therapeutic benefits (Gallucci et al., 2009; Yue et al., 2021). Since our aim was to look for biocompatible green compounds, we chose these commonly available food-grade aromas with conventional terpenes. Table S1 lists the various compositions of the binary mixtures tested at molar ratios ranging from 1:9 to 9:1 and highlights the ones that resulted in the successful formation of hydrophobic DESs. Table 2 depicts the components of the optimised DESs, which were used for subsequent emulsification studies, and their physicochemical properties like melting point, water content, density, and refractive index.

As seen in Table 2, three different DESs, namely, menthol:vanillin, menthol:raspberry ketone, and thymol:raspberry ketone, were screened at nine different molar compositions for the preparation of hydrophobic DESs. Higher amounts of menthol were required for the successful formation of hydrophobic DESs when tested with vanillin. Contrarily, the replacement of vanillin with raspberry ketone seems to lead to the formation of hydrophobic DESs in all tested molar compositions. Meanwhile, there seems to be no clear profile in the molar compositions of thymol and raspberry ketone, except that the possibility of obtaining hydrophobic DESs seems to be higher when thymol is mixed in larger quantities with raspberry ketone. Lastly, the presence of water in such small quantities in the prepared hydrophobic DESs reaffirms the hydrophobic nature of the eutectic mixtures. Also, the DESs listed in Table 2, were stored at 25°C in sealed vials and found to be stable for over a year.

In accordance with the primary objective of using these hydrophobic DESs as dispersed phases for the formulation of DES-in-water nanoemulsions for biomedical applications, the highest possible amounts (9:1 M ratio) of stronger antimicrobial agents (menthol & thymol) in the DESs were chosen for further characterisation studies. The three optimised hydrophobic DESs are referred to as DES A, DES B, and DES C (as in Table 2) throughout the manuscript.

As expected, the densities of all the three hydrophobic DESs were

**Table 2**  
Characterisation of the three selected hydrophobic DESs.

DES sample	Melting point [°C]	Water content [wt. %]	Density [g. ml <sup>-1</sup> at 25 °C]	Refractive index [ $\times 10^{-6}$ ]
DES A (Menthol: vanillin 9:1)	27.23	<1.00	0.888 ± 0.006	1.47
DES B (Menthol: raspberry ketone 9:1)	26.09	<0.90	0.799 ± 0.009	1.46
DES C (Thymol: raspberry ketone 9:1)	43.36	<0.60	0.987 ± 0.010	1.52

lower than water, and the DES with thymol seem to have a higher value in comparison to menthol-based, as the intrinsic density of thymol is higher than that menthol (see Table 1). Lastly, the formation of DESs was characterised in terms of DSC studies (for graphs, see Table S2), as the phase transitions of the DESs show a melting point much lower than their solid hydrophobic components. We named the eutectic mixtures as “deep” as the melting points of the DESs were much smaller than that of the aroma-based compounds. Although the peak melting points were  $\sim 27$ ,  $26$  and  $43$  °C (DES A, B and C respectively), it can be clearly seen in the DSC plots that the crystallization points were much lower and hence the mixtures were very stable until much lower temperatures than the peaks.

Fig. 2 depicts a semi-log plot of the dynamic viscosities of these three DESs as a function of temperature. As expected, the viscosity reduces with the increase in temperature. Notably, the viscosities around  $25$  °C of all three DESs were feasible for membrane emulsification, allowing for relatively mild operating pressures ( $\sim 0.2$  bar) in the membrane emulsification unit. Out of the three prepared DESs, the viscosity of DES C at  $25$  °C was lower than DES B and DES A by 63% and 68% respectively.

### 3.2. Formulation of DES-in-water nanoemulsions by membrane emulsification

The present study aims at formulating monomodal DES-in-water nanoemulsions with reduced size dispersity. The three selected DESs were dispersed at varying concentrations of 2%, 4% and 6% that correspond to 1 ml, 2 ml, and 3 ml of the dispersed phase, respectively, for producing 50 ml of emulsion. Each dispersed phase was injected at the flowrates,  $Q_D$ , of  $0.05$  ml  $\text{min}^{-1}$  and  $0.1$  ml  $\text{min}^{-1}$ . As mentioned before, the continuous phase was recirculated at a  $Q_C$  of  $150$  ml  $\text{min}^{-1}$  which was the maximum operating capacity of the peristaltic pump used. This corresponds to a crossflow velocity  $v_c$  of  $0.32$  m  $\text{s}^{-1}$ . Fig. 3 illustrates the DLS profiles and TEM images of the optimised nanoemulsions formulated by using DES A, DES B, and DES C, at controlled dispersed phase concentrations and flowrates. Furthermore, Table S3 of the supplementary material compiles the results of all these membrane emulsification-based experiments in terms of  $Z_{\text{avg}}$  mean droplet size (nm) and polydispersity index PDI (–) of the produced emulsions.

As seen in Fig. 3 and as detailed in Table S3, all three DESs were able to produce nanoemulsions having a maximum of 4% (v/v) of the dispersed phase. At 6% (v/v), the emulsions had undesirably high PDI values ( $\sim 0.7$ – $1.0$ ), indicating polydispersity. The emulsions with DES A and DES B didn't produce mono-modal distributions at all tested dispersed phase concentrations and flowrates. The selected DES A- and DES B-based nanoemulsions of  $Z_{\text{avg}} = 37.4$  nm  $\pm$  0.8 nm and  $221.4$  nm  $\pm$  51.6 nm sizes respectively, were formulated at 4% (v/v) dispersed phase and  $0.1$  ml  $\text{min}^{-1}$  of dispersed flowrate. On the contrary, the DES

C-in-water nanoemulsion at 4% (v/v) dispersed phase and  $0.05$  ml  $\text{min}^{-1}$  of flowrate was able to formulate monomodal distribution with  $Z_{\text{avg}} = 146.5$  nm  $\pm$  0.3 nm and PDI = 0.22. The sizes and distributions of the nanoemulsions were complimented by TEM analysis. Notably, for DES A-based nanoemulsion some larger aggregates can be seen in the backdrop of the TEM image. An interesting observation was made wherein the bulk of the emulsion droplets comprising of menthol (DES A and DES B) seem to be populated around 40 nm–60 nm. On the other hand, thymol-based emulsions (DES C) were of slightly larger sizes. Similar observations were reported in literature wherein these DES-in-water nanoemulsions were produced by ultrasound and membrane emulsification techniques (Syed et al., 2020, 2022; Zeng et al., 2021). Another interesting observation was that we were able to produce emulsion droplets which were 99.5%, 97.5%, and 98.4% smaller than the membrane pore size of  $9$   $\mu\text{m}$  for DES A, B and C respectively. Thus, this process may be redefined as a membrane-assisted nanoemulsification technique as membrane pores are assisting rather than control the size of the emulsion droplet (Syed et al., 2020). Lastly, with these unique chemical attributes of the DESs, the characterisations of the interfacial tension and wetting properties of the DESs involved are required.

### 3.3. Characterisation of the two phases and the membrane used to produce DES-in-water nanoemulsions

The pendant drop method was used to quantify the effect of surface-active agents such as surfactants in lowering the interfacial tension between the continuous phase and dispersed phase. Tween 80 surfactant is reported as an effective surfactant with a hydrophilic-lipophilic balance (HLB) value of 15 to form oil-in-water emulsions. As seen in Fig. 4(A), Tween 80 surfactant was able to reduce the interfacial tension of the continuous phase with DESs by  $\sim 70\%$  when compared to Milli-Q water with DESs.

An interesting phenomenon was further observed in the results presented in Fig. 4(A). Usually, the oils used in the formulation of oil-in-water emulsions such as corn oil, olive oil, grapeseed oil, coconut oil, etc., have interfacial tension values in the range of  $23$ – $26$  mN  $\text{m}^{-1}$  (Mondal et al., 2022; Fisher et al., 1985). DES A and B in contact with water exhibit interfacial tensions of similar values as the alimentary oils, however, the interfacial tension of DES C in contact with water is much lower ( $15.83$  mN  $\text{m}^{-1}$ ). Although this is a hydrophobic solvent, such low values of interfacial tensions with water need further investigations which are out of the scope of this study.

For any given membrane emulsification process it is imperative that the continuous phase wets the membrane surface to facilitate droplet detachment (Charcosset et al., 2004; Piacentini et al., 2014). As seen in Fig. 4(B) the static contact angle of water with the stainless-steel membrane was  $51.3^\circ \pm 0.9^\circ$ , signifying hydrophilicity. Interesting results were observed for all three selected DESs as they wet the membrane surface despite being hydrophobic. As reported by Syed et al. in earlier works, irrespective of the composition of the hydrophobic DESs, they have an intrinsic wetting property on the membrane surfaces (Syed et al., 2022). This unique surface chemistry aspect of DESs could result in cost-saving at an industrial scale as negligible transmembrane pressures are required to formulate DES-in-water nanoemulsions.

Certain unique anomalies like nanoemulsion droplets were formed despite using a microporous membrane. As the DESs were wetting the active membrane surface, a layer might be formed on it. Thereafter, due to the high continuous shear rate from the aqueous phase, nanodroplets might be dragged off the deposited layer. Furthermore, there could be other physicochemical properties of these DESs that need to be investigated by advanced tools such as molecular dynamic simulations to better understand the “shrinkage” of the droplets. Nevertheless, attempts had been made to understand the spatial molecular orientation of the individual molecules in DES using advanced NMR techniques (see section 3.5) to further elucidate this behaviour.

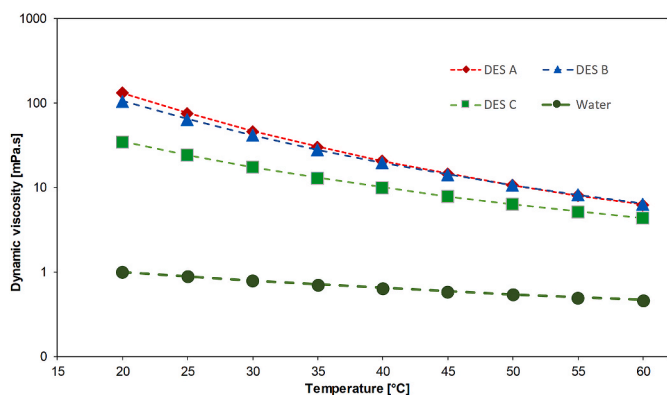
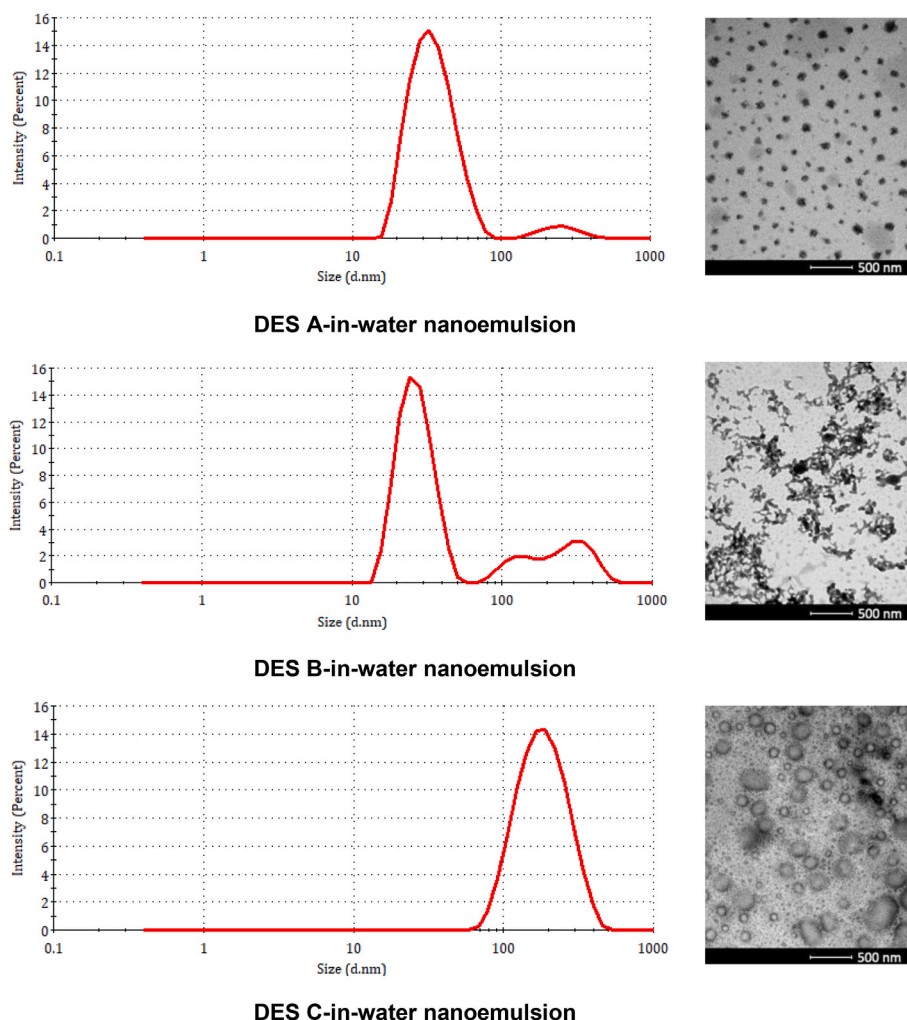


Fig. 2. Plot of dynamic viscosities of the three selected DESs as a function of temperature.



**Fig. 3.** Emulsion size and size distribution of the optimised DES-in-water nanoemulsions characterised by DLS and TEM. **A.** DES A-in-water nanoemulsion ( $0.1 \text{ ml min}^{-1}$  DP flowrate) **B.** DES B-in-water nanoemulsion ( $0.1 \text{ ml min}^{-1}$  DP flowrate) **C.** DES C-in-water nanoemulsion ( $0.05 \text{ ml min}^{-1}$  DP flowrate). **NOTE:** All three reported DESs were formulated at 4% dispersed phase (DP) concentrations.

### 3.4. Antimicrobial studies of the therapeutic DES-in-water nanoemulsions

The aroma compounds-based hydrophobic DES-in-water nanoemulsions were subjected to antibacterial and antifungal studies. Previously, antibacterial studies with hydrophobic DES and hydrophobic DES-based emulsions have been reported for menthol- and thymol-based DESs (Syed et al., 2020; Usman T Syed et al., 2022; Zeng et al., 2021). The antifungal activities of hydrophobic DES-based emulsions are explored for the first time in this study. Table 4 and S5 respectively depict the results from the antibacterial and antifungal studies performed. It must be noted that to increase the solubility of the four individual hydrophobic compounds, the stock solutions had to include Tween 80 when determining the MIC and MBC/MFC values against the below-mentioned microorganisms.

#### 3.4.1. Antibacterial studies

The antibacterial properties of the selected DESs, their individual components, and the optimised nanoemulsions were studied against 1 g-positive *S. aureus* strain and 1 g-negative *E. coli* strain and Table 3 depicts the MIC and MBC values obtained.

The role of low concentrations of Tween 80 in the overall formulation of the nanoemulsion was not for any significant therapeutic effect but to reduce the interfacial tension between the two immiscible phases of the emulsions (Syed et al., 2021). As seen in Table 3, the Tween 80 surfactant did not exhibit any kind of inhibitory effect for both bacterial

strains, up to the maximum concentration tested ( $153.6 \text{ mg ml}^{-1}$  of Tween 80), which exonerates this compound from contributing to the antimicrobial activity observed and discussed below. Regarding the results obtained with the *S. aureus* bacterial strain, vanillin ( $3.5 \text{ mg ml}^{-1}$ ) and menthol ( $3.8 \text{ mg ml}^{-1}$ ) are the most effective among the four individual hydrophobic compounds in inhibiting the growth of bacteria, with very similar behaviours, while menthol shows enhanced bactericidal properties when compared to vanillin (effective amount of menthol needed for bactericidal effect was  $3.8 \text{ mg ml}^{-1}$  and  $13.9 \text{ mg ml}^{-1}$  for vanillin). The third most active compound was thymol, showing bactericidal activity at a slightly higher concentration,  $17.6 \text{ mg ml}^{-1}$ . Raspberry ketone seems to be the least effective individual compound tested towards the target *S. aureus* strain. Although menthol and vanillin were individually effective against *S. aureus*, their eutectic mixture (DES A) was not as effective since it required more menthol ( $32.0 \text{ mg ml}^{-1}$ ) in the mixture to achieve the same effect. The combination of menthol and raspberry ketone (DES B), seems to be more effective than DES A as the MIC value of DES B was 2 times lower than DES A while the MBC value was 4 times lower. Lastly, the most effective and desirable antibacterial results of all tested DESs were seen for DES C comprising thymol and raspberry ketone. When tested individually, thymol and raspberry ketone had lower antibacterial activity with MIC values of  $4.4$  and  $15.2 \text{ mg ml}^{-1}$ , respectively, and MBC values of  $17.6 \text{ mg ml}^{-1}$  and  $>30.5 \text{ mg ml}^{-1}$ , respectively. Nonetheless, when these were in a eutectic mixture (DES C), they were the most bacteriostatic, with a MIC of  $3.9 \text{ } \mu\text{l ml}^{-1}$ , and

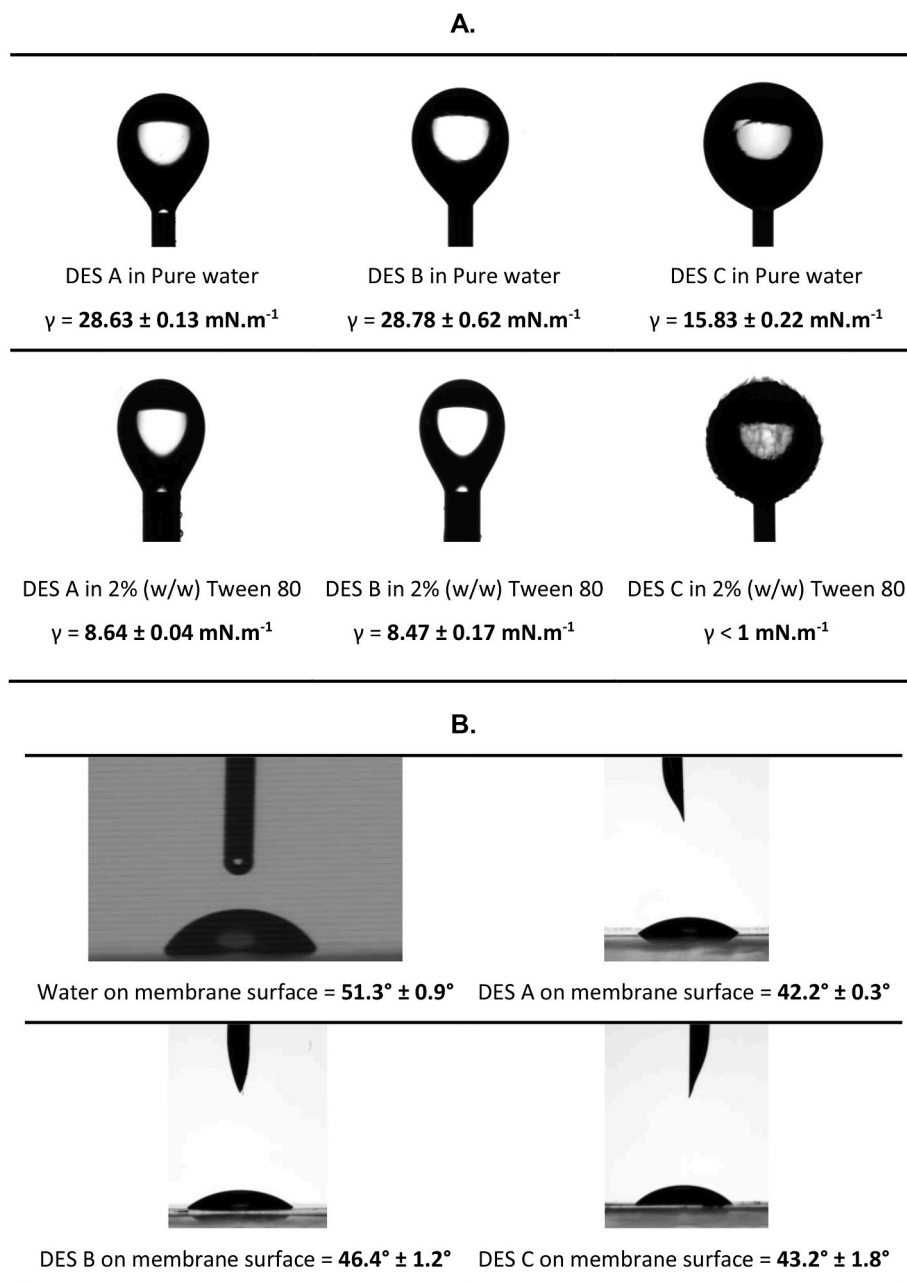


**Fig. 4.** Characterisation of the phases involved: **A.** Interfacial tension between the two phases and **B** Static contact angles of water and the selected DESs on the membrane surface.

bactericidal, with an MBC value of  $15.6 \mu\text{l ml}^{-1}$ . These attributes of DES C could be a result of the synergetic effect of these two compounds to exhibit antibacterial properties against the target *S. aureus* strain.

This study aimed to reduce the amounts of hydrophobic compounds required to produce competitive therapeutic effects by formulating nanoemulsions. As seen in Table 3, despite the MIC and MBC of DES C-in-water nanoemulsions being the same when compared to the DES C, around 15 times less of each individual compounds, thymol, and raspberry ketone, were used. Similar results were observed for DES A and DES B-based nanoemulsions. The MIC and MBC of DES A-in-water nanoemulsions were reduced by 4 and 16 times, respectively, when compared to DES A. The individual compounds of menthol and vanillin present in the DES A-based nanoemulsions at the MBC value were lesser than 250 times each when compared to their amounts in DES A. The MIC and MBC of DES B-in-water nanoemulsions were both reduced by 2 times when compared to the DES B. The individual compounds of

menthol and raspberry ketone present in the DES B-based nanoemulsions at the MBC value were lesser than 25 times each when compared to their amounts in DES B. DES C-in-water nanoemulsion exhibited, nonetheless, the best bacteriostatic and bactericidal activities.

Additionally, DES C formed a more uniform nanoemulsion as exhibited in section 3.2. The enhanced antibacterial effects of nanoemulsions could be attributed to their increased specific surface area (whereby the contact of the bacterial surface with the antimicrobial agent would be increased) and it would also promote better bioavailability and mass transport of the biocidal agents (Usman T Syed et al., 2022; Zeng et al., 2021).

The antibacterial results shown in Table 3 for the Gram-negative bacteria, *E. coli*, clearly suggest that hydrophobic terpenes (menthol and thymol) are more effective against Gram-positive bacteria such as *S. aureus*. Similar results were witnessed previously in literature as Gram-negative bacteria such as *E. coli* possess an outer membrane

**Table 3**

Determination of the MIC and MBC values for the individual components, the prepared DESs, and the optimised emulsions produced by membrane-assisted nanoemulsification against *Staphylococcus aureus* ATCC 6538 and *Escherichia coli* ATCC 8739 bacterial strains. NOTE: R. ketone signifies raspberry ketone.

Bacteria	Sample	MIC ( $\mu\text{l}$ of testing sample. $\text{ml}^{-1}$ )	Sample composition at MIC value					MBC ( $\mu\text{l}$ of testing sample. $\text{ml}^{-1}$ )	Sample composition at MBC value				
			[Tween 80] $\text{mg.ml}^{-1}$	[Menthol] $\text{mg.ml}^{-1}$	[Thymol] $\text{mg.ml}^{-1}$	[Vanillin] $\text{mg.ml}^{-1}$	[R.ketone] $\text{mg.ml}^{-1}$		[Tween 80] $\text{mg.ml}^{-1}$	[Menthol] $\text{mg.ml}^{-1}$	[Thymol] $\text{mg.ml}^{-1}$	[Vanillin] $\text{mg.ml}^{-1}$	[R.ketone] $\text{mg.ml}^{-1}$
<i>S. aureus</i> ATCC 6538	Tween 80	> 500.0	> 153.6					> 500.0	> 153.6				
	Menthol	7.8	0.1	3.8				7.8	0.2	3.8			
	Thymol	7.8	0.1		4.4			31.3	0.6		17.6		
	Vanillin	62.5	1.2			3.5		250.0	4.8			13.9	
	R. ketone	250.0	4.8				15.2	> 500.0	> 9.6				> 30.5
	DES A	62.5		32.0		3.5		250.0		128.2		13.9	
	Nanoemulsion A	15.6	0.3	0.5		0.0(5)		15.6	0.3	0.5		0.0(5)	
	DES B	31.3		14.3			1.7	62.5		28.6			3.3
	Nanoemulsion B	15.6	0.3	0.4			0.0(5)	31.3	0.6	1.1			0.1
	DES C	3.9			2.2		0.3	15.6			8.8		1.1
	Nanoemulsion C	3.9	0.0(8)		0.1		0.0(2)	15.6	0.3		0.6		0.0(7)
<i>E. coli</i> ATCC 8739	Tween 80	> 500.0	> 153.6					> 500.0	> 153.6				
	Menthol	> 500.0	> 9.6	> 242.6				> 500.0	> 9.6	> 242.6			
	Thymol	62.5	1.2		35.2			62.5	1.2		35.2		
	Vanillin	62.5	1.2			3.5		62.5	1.2			3.5	
	R. ketone	250.0	4.8				15.2	250.0	4.8				15.2
	DES A	250.0		128.2		13.9		250.0		128.2		13.9	
	Nanoemulsion A	500.0	9.6	16.0		1.7		500.0	9.6	16.0		1.7	
	DES B	125.0		57.2			6.7	125.0		57.2			6.7
	Nanoemulsion B	> 500.0	> 9.6	> 14.3			> 1.7	> 500.0	> 9.6	> 14.3			> 1.7
	DES C	15.6			8.8		1.1	15.6			8.8		1.1
	Nanoemulsion C	15.6	0.3		0.5		0.0(7)	15.3	0.3		0.6		0.0(7)

composed of inner phospholipids and outer lipopolysaccharides. The hydrophilic part of lipopolysaccharides with a negative charge is the external part of the cell, the surface. The porins are proteins that make channels for hydrophilic compounds to cross the outer membrane. The permeability of the outer membrane is poor for hydrophobic compounds and charged compounds (Cama et al., 2019).

On the other hand, the aroma-based compounds (vanillin and raspberry ketone) presented better bactericidal properties against *E. coli* when compared to *S. aureus*. Although a detailed study of the mechanism of action could prove beneficial for understanding the antibacterial effect, it is out of the scope of the current study. Furthermore, there is a possibility that the porins assisted in the transportation of these aroma compounds across the outer membrane of the bacterial cell wall as they have a relatively higher hydrophilic character in comparison to terpenes (Shu et al., 2017). Moreover, in our previous studies, we had reported that menthol and decanoic acid, and menthol and thymol based DESs-in-water nanoemulsions were ineffective and slightly effective, respectively, against the *E. coli* strain (Syed et al., 2020; Usman T Syed et al., 2022). These results are depicted in Table S4 of the supplementary material. DES A- and DES B-based nanoemulsions with menthol did not present any enhanced antibacterial action against *E. coli*, however, DES C-in-water nanoemulsions with thymol proved to be highly efficient. When compared to the *S. aureus* assay, the MBC values were identical, while MIC values were slightly higher but still the most effective of the nanoemulsions tested. Thus, it could be safely concluded that thymol and raspberry ketone-based DES C-in-water nanoemulsions could be selected as the best candidate for therapeutic applications and the same concentration of  $15.63 \mu\text{l ml}^{-1}$  is bactericidal for *S. aureus* and *E. coli*.

### 3.4.2. Antifungal studies

Table 4 depicts the antifungal studies of the components of DES C,

DES C and DES C-based nanoemulsion against four different fungal strains. As seen in Table 4, all the individual compounds were active against fungi, particularly thymol (Minimum Fungicidal Concentration (MFC) of  $0.2\text{--}1.9 \mu\text{l ml}^{-1}$ ). Highlighted antifungal properties with DES C-based emulsions can be seen in Table 4, while the detailed results are compiled in the supplementary material (Table S5). As expected, Tween 80 did not exhibit an inhibitory effect on fungi until  $250.0 \mu\text{l ml}^{-1}$ . Thymol exhibited more fungicidal activity when compared to raspberry ketone as the MFC values were 65–255 times lower. Although both these compounds were more effective against *T. mentagrophytes* (a dermatophyte filamentous fungus) when compared to *Candida* species (yeasts), higher quantities of both were needed to exhibit fungicidal effect against the filamentous fungus *A. fumigatus*. It is well-established that thymol is effective against skin disorders and hence, it is effective against dermal-related bacteria such as *Cutibacterium acnes* or even dermatophyte fungi like *T. mentagrophytes* (Escobar et al., 2020; Kowalczyk et al., 2020; Vale-Silva Maria José; Cavaleiro, Carlos; Salgueiro, Lúcia; Pinto, Eugénia, 2010).

The MFC values of the DES C against all four fungal strains seem to be rather low when compared to the DES C-in-water nanoemulsion (8–65 times). Enhanced antifungal properties of DES C and its corresponding nanoemulsions were witnessed against *A. fumigatus*, the species less susceptible to individual thymol and raspberry ketone; the amounts of thymol and raspberry ketone were reduced by half and 218 times compared to their nanoemulsion state. This synergistic effect reflects lesser amounts of components required for fungicidal action leading to cost reduction. Moreover, it also substantiates its usage for therapeutic application as hydrophobic components cannot be easily used in a polar environment and they need to be dispersed in an emulsion system. Furthermore, the cytotoxicity studies carried out in literature indicate that the toxicity levels are greatly reduced if the DES components are

**Table 4**

Determination of MIC and MFC for the individual components; DES C; and the optimised emulsion produced by membrane-assisted nanoemulsification against: *Candida albicans* ATCC 10231, *Candida krusei* ATCC 6258, *Aspergillus fumigatus* ATCC 204305, and *Trichophyton mentagrophytes* FF7 fungal strains. NOTE: R. ketone signifies raspberry ketone.

Microorganism	Sample	MIC ( $\mu\text{l}$ of testing sample. $\text{ml}^{-1}$ )	Sample composition at MIC value			MFC ( $\mu\text{l}$ of testing sample. $\text{ml}^{-1}$ )	Sample composition at MBC value		
			[Tween 80] $\text{mg.ml}^{-1}$	[Thymol] $\text{mg.ml}^{-1}$	[R. ketone] $\text{mg.ml}^{-1}$		[Tween 80] $\text{mg.ml}^{-1}$	[Thymol] $\text{mg.ml}^{-1}$	[R. ketone] $\text{mg.ml}^{-1}$
<i>Aspergillus fumigatus</i> ATCC 204305	Tween 80	> 500.0	> 153.6			> 500.0	> 153.6		
	Thymol	0.5	0.0(1)	0.3		1.9	0.0(4)	1.1	
	R. ketone	31.3	0.6		1.9	250.0	4.8		15.2
	DES C	0.5		0.3	0.0(3)	1.9		1.1	0.1
	<b>Nanoemulsion C</b>	<b>7.8</b>	<b>0.2</b>	<b>0.3</b>	<b>0.0(3)</b>	<b>15.6</b>	<b>0.3</b>	<b>0.6</b>	<b>0.0(7)</b>
<i>Candida albicans</i> ATCC 10231	Tween 80	> 500.0	> 153.6			> 500.0	> 153.6		
	Thymol	0.2	0.0(1)	0.1		0.5	0.0(1)	0.3	
	R. ketone	31.3	0.6		1.9	62.5	1.2		3.8
	DES C	0.2		0.1	0.0(2)	1.0		0.6	0.0(7)
	<b>Nanoemulsion C</b>	<b>3.9</b>	<b>0.0(8)</b>	<b>0.1</b>	<b>0.0(2)</b>	<b>7.8</b>	<b>0.2</b>	<b>0.3</b>	<b>0.0(3)</b>
<i>Candida krusei</i> ATCC 6258	Tween 80	> 500.0	> 153.6			> 500.0	> 153.6		
	Thymol	0.5	0.0(1)	0.3		0.5	0.0(1)	0.3	
	R. ketone	62.5	1.2		3.8	125.0	2.4		7.6
	DES C	0.5		0.3	0.0(3)	1.0		0.6	0.0(7)
	<b>Nanoemulsion C</b>	<b>7.8</b>	<b>0.2</b>	<b>0.3</b>	<b>0.0(3)</b>	<b>15.6</b>	<b>0.3</b>	<b>0.6</b>	<b>0.0(7)</b>
<i>Trichophyton mentagrophytes</i> FF7	Tween 80	250.0	76.8			> 500.0	> 153.6		
	Thymol	0.2	0.0(1)	0.1		0.2	0.0(1)	0.1	
	R. ketone	15.6	0.3		0.9	15.6	0.3		0.9
	DES C	0.1		0.0(7)	0.0(08)	0.1		0.0(7)	0.0(08)
	<b>Nanoemulsion C</b>	<b>3.9</b>	<b>0.0(8)</b>	<b>0.1</b>	<b>0.0(2)</b>	<b>7.8</b>	<b>0.2</b>	<b>0.3</b>	<b>0.0(3)</b>

emulsified and present in dilute medium (Usman T Syed et al., 2022; Zeng et al., 2021). As seen in Table S5 of supplementary material, when compared to other emulsion systems, thymol, and raspberry ketone-based DES C-in-water nanoemulsions clearly seem to be more potent against the fungal strains.

Although this was the first study to report the antifungal benefits of hydrophobic DESs-in-water nanoemulsions, yet it could be interesting to compare these MFC values with the other reported hydrophobic/hydrophilic counterparts of the DESs. For all the three tested DESs-in-water nanoemulsions, the amount of individual fungicidal agents required is lesser than those tested by Gao et al., wherein they reported novel carbon dots-based hydrophilic DESs comprising of choline chloride and urea against *C. albicans* fungal strain (Gao et al., 2019). This fungal strain was also tested by Silva et al., in 2019 wherein the DESs were comprised of various fatty acids. In this study too, the individual components seem to perform better than their corresponding DESs (Silva et al., 2019). However, as seen by Tables 4 and S5, the terpenes-based DESs seem to perform better against *C. albicans* than the fatty acids-based DESs. These results were also comparable with the recent work of Silva et al., wherein menthol and thymol were used to produce DESs with the non-steroidal anti-inflammatory ibuprofen drug and tested against *C. albicans* fungal strain (Silva et al., 2021). The other works do not directly use DESs as therapeutic agents to tackle fungi, instead, they use DES either to extract from plants and other compounds functional derivatives with antifungal action or as vehicles loaded with antifungal bioactive agents (Bušić et al., 2020; Espino et al., 2019; Jin et al., 2019).

Thus, this study reaffirms the potentiality of exploring nanoemulsions made from hydrophobic therapeutic DESs for enhanced antimicrobial activities to treat infection involving bacteria or fungi. Still, the biocompatibility of the nanoemulsions needs to be tested before

practical use. However, considering the natural origin of the starting materials and sustainability of the employed processes, it can be safely predicted that these DESs and DES-based nanoemulsions can be seen as a potential alternative to existing antimicrobial agents. To sum up, DES C is more active against fungi than DES C-in-water nanoemulsions, but it should be noted that the same concentration of  $15.6 \mu\text{l ml}^{-1}$  is bactericidal for *S. aureus* and *E. coli* and fungicidal for *Candida*, *Aspergillus* and  $7.8 \mu\text{l ml}^{-1}$  for the dermatophyte tested.

### 3.5. Structural analysis of DESs and emulsions using advanced NMR techniques

NMR spectroscopy has become a very powerful technique in DES research. NMR experiments are mainly focused on structural analysis, but they can also provide information on both dynamics and interactions at the molecular level (Häkkinen et al., 2019). Among the latter, it is worth noting the experiments based on diffusion and the nuclear overhauser effect (NOE) (Hansen et al., 2021).

To verify the composition of the DESs,  $^1\text{H}$  NMR and  $^{13}\text{C}$  NMR experiments were performed on pure samples. The peaks attributed to the individual compounds were clearly identified and no new peaks were detected (as seen in Supplementary Fig. S4) thereby ruling out the possibility of a chemical reaction between the two components. NMR experiments based on the Nuclear Overhauser (namely NOESY and ROESY) have been recorded to elucidate the structural orientation of components: two nearby protons ( $<5 \text{ \AA}$ ) will give a "cross-peak" in the two-dimensional spectrum on either side of the diagonal. By agreement, the sign of the diagonal is negative. The sign of a NOESY cross-peak depends, among other factors, on the rate at which the molecule tumbles in solution and therefore, on the molecular weight. For small molecules NOESY cross-peaks are positive, while for larger molecules are

negative, the same as the exchange peaks. So, to identify the exchange peaks, a ROESY spectrum must be recorded since the latter will appear negative, while the cross-space interactions will always be positive peaks. These experiments allow to detect inter and intramolecular interactions between nuclei (protons) close in space as illustrated in Fig. 5.

DES A and DES B exhibit similar characteristics: in both NOESY spectra, there are cross-peaks between almost all proton signals, indicating the existence of a strong interaction between different species throughout space. In addition, all the signals observed are negative (of the same sign as the diagonal), which suggests the formation of a supramolecular structure. ROESY experiments reveal that the hydroxyl proton of phenol is in chemical exchange with the hydroxyl proton of menthol (see in supplementary materials Fig. S5).

On the contrary, DES C presents some differences in the  $^1\text{H}$  spectrum, wherein, three signals attributed to OHs are observed, one of them around 3.15 ppm assigned to “free OH”. Furthermore, in the NOESY spectrum of DES C (see supplementary materials Fig. S6) the few cross-peaks observed are positives and indicate intramolecular interactions. The only negative peaks are the ones corresponding to chemical exchange between the OHs. In this case the interaction between thymol and raspberry ketone is weaker and did not form a supramolecular structure. The contact was established only through the hydroxyl groups. Thus, components of DES C are bound in such a way that creates more free volume than DESs A and B. These spatial cavities can accommodate water molecules and thus the interfacial tension of DES C (despite being hydrophobic) in contact with water is much lower than DESs A and B.

As DES C was optimised in our earlier antifungal studies, the aforementioned NMR techniques were employed to further investigate the structural studies of DES C-in-water nanoemulsions and its constituents (namely, Tween 80 surfactant and DES C). As Fig. 6 depicted the  $^1\text{H}$  NMR spectra, the  $^1\text{H}$  signals from Tween 80 appear clearly at lower frequency (Fig. 6, dashed arrows). These changes can be attributed to the shielding effect of both thymol and raspberry ketone aromatic rings (ring current-induced shift) assuming that these molecules remain solubilized in the core of the emulsion. Thus, a new signal of ethylene groups of polyethylene oxide (PEO) appears at 3.25 ppm in the emulsion, although the initial signal can also be seen at 3.7 ppm. This shift of the peak could be attributed to the “free PEO groups” or it could indicate the existence of a balance between the Tween 80 micelles and the emulsion, based on the diffusion coefficients determined by  $^1\text{H}$  DOSY experiments (see Fig. S7 of supplementary material) (Awad et al., 2018). These results are in agreement with the studies carried out by Awad et al., in which the coexistence of aggregates of different sizes in solution was demonstrated (Awad et al., 2018).

For further understanding of the inter and intramolecular interactions within the emulsion, 2D NOESY experiments were performed. As seen in Fig. 7, the negative sign of all cross-peaks supports the existence of supramolecular aggregates of DES C and Tween 80 (slow rotational tumbling). These experiments with the emulsion were performed at a mixing time of 200 ms. To rule out that the crossing peaks

are due to diffusion problems, 2D ROESY experiments were also performed (see the spectra in Fig. S8 of the supplementary material). The cross-peaks were positive with a sign opposite to the diagonal although less intense than in NOESY.

A closer examination of Fig. 7 depicting the 2D spectra of the NOESY experiment suggests that all the aromatic protons of thymol (c, f, d) have NOE interactions with the (i) hydrophilic polyethylene oxide groups, (ii) the protons of the main chain ( $-\text{CH}_2-$ ), (iii) end methyl group of the aliphatic chain (18) of Tween 80. The interaction of the aliphatic protons of the thymol molecule (h, i) with the hydrophobic protons of Tween 80 cannot be detected due to the overlapping of said signals, although some weak cross-peaks can be seen between g and 11, 12, 15, 18 and  $-\text{CH}_2$ . The signals of the raspberry ketone molecule are barely visible but cross-peaks can be seen between the protons F, G, D, C and those of polyethylene oxides (pointed by black arrows). There are also intermolecular NOE interactions between the DES molecules (highlighted by black circles). From these data and from the observation that thymol has the same diffusion coefficient as Tween 80 (DOSY experiment, Fig. S7), it could be deduced that thymol molecules are in the core of the emulsion. Also, it can be suggested that the raspberry ketone got attached with the hydrophilic cell walls of the microbes and leads the thymol to permeate through the membranes, ultimately resulting in breakage of the cytoplasmic membrane. This might be the possible mechanism of enhanced antimicrobial activity of this DES and nanoemulsions against the selected bacterial and fungal strains.

#### 4. Conclusions

This work presents the formulation of three novel hydrophobic DESs by combining terpenes (menthol or thymol) and aroma-based compounds (vanillin or raspberry ketone). Thereafter, an energy efficient membrane-assisted nanoemulsification technique was employed to formulate DES-in-water nanoemulsions using laser-drilled isoporous metallic membranes. It was interesting to note the fact that although a microporous membrane was used, nanoemulsions were formed. Unique physicochemical properties such as reduced interfacial tension between the hydrophobic DES and aqueous phase and the wetting properties of hydrophobic DES on a hydrophilic membrane surface were observed. This led to the hypothesis that instead of conventional droplet detachment in membrane emulsification, hydrophobic DES might form a layer on the active side of the membrane which was subsequently ripped out in the form of nanoemulsion droplets due to the high shear rate of the continuous phase. Alternatively, there could be a possible “shrinkage” of the hydrophobic DES in the presence of aqueous media which can be better understood by studying the molecular dynamic simulations of the DES, water, and surfactant interactions.

From an experimental perspective, with an optimised dispersed phase flowrate  $Q_{\text{DP}}$  of  $0.05 \text{ ml min}^{-1}$ , a continuous phase velocity  $v_c$  of  $0.32 \text{ m s}^{-1}$ , using isoporous stainless steel membrane (active side pore diameter of  $9 \mu\text{m}$  & pore pitch of  $100 \mu\text{m}$ ), DES-in-water nanoemulsions were formed. DES C-based nanoemulsion, containing thymol and

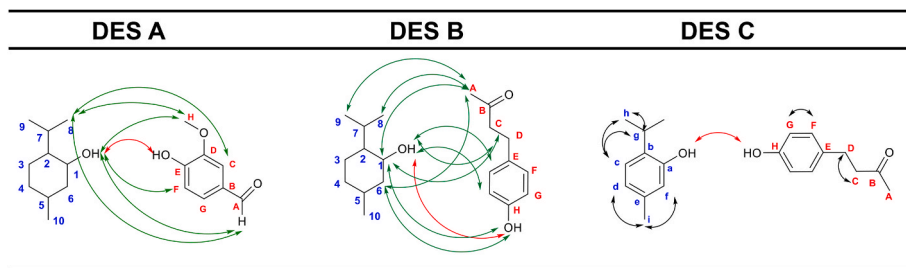


**Fig. 5.** Structural orientation of DESs as determined by NOESY & ROESY (Green arrows represent intermolecular interactions, black arrows represent intramolecular interactions and red arrows represent phenolic  $-\text{OH}$  bond interactions). (For interpretation of the references to colour in this figure legend, the reader is referred to the Web version of this article.)

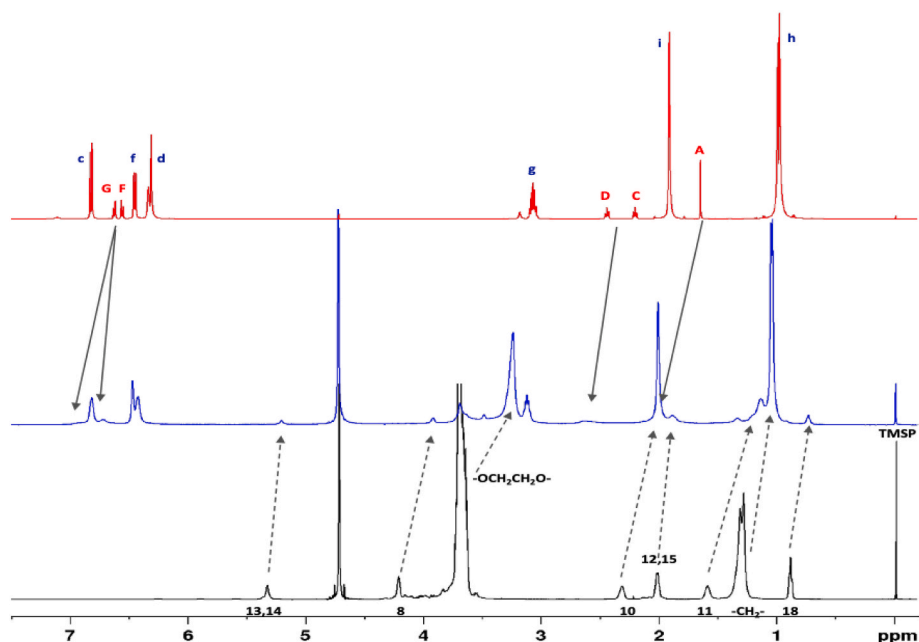


**Fig. 6.** Comparative  $^1\text{H}$  NMR spectra of DES C (in red), emulsion (in blue) and Tween 80 (in black). See Fig. S3B for the assignment of the Tween 80 signals. (For interpretation of the references to colour in this figure legend, the reader is referred to the Web version of this article.)

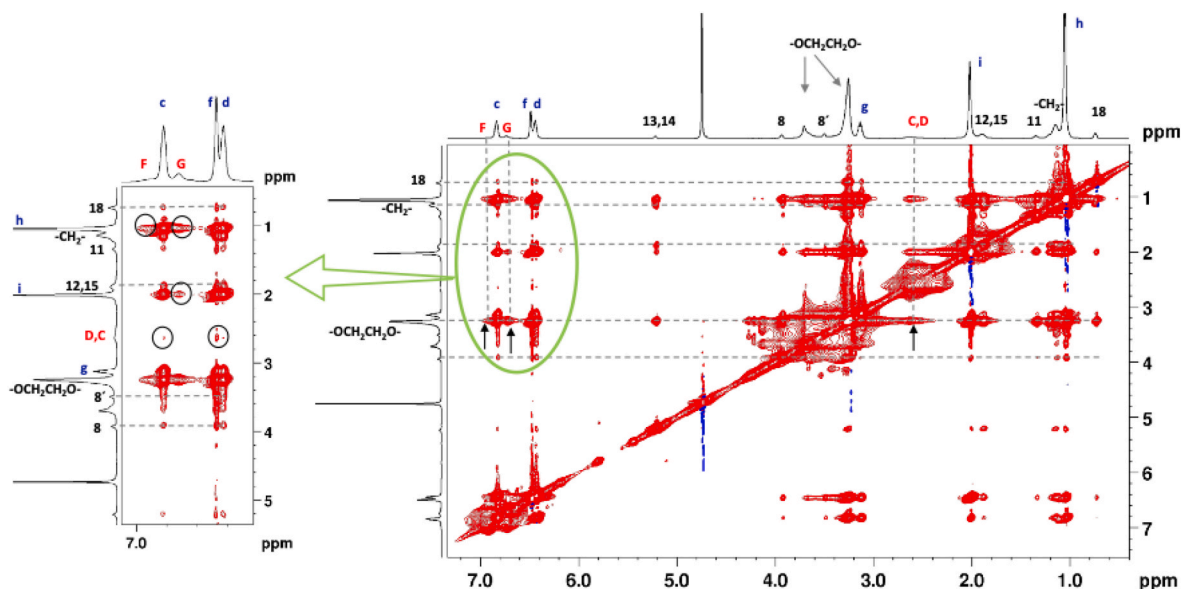


**Fig. 7.**  $^1\text{H}$  NOESY spectrum of DES C based nanoemulsion and its zoom-in of the spectral area of interest to determine inter and intramolecular interactions of nuclei in close space. ( $t_{\text{mix}} = 200$  ms).

raspberry ketone, exhibited a monomodal distribution with a droplet size of  $146.5 \text{ nm} \pm 0.3 \text{ nm}$  and a PDI of 0.22. The DES-in-water nanoemulsions were tested for their antimicrobial activities. They showed stronger antibacterial properties against the target *S. aureus* than *E. coli*. Also, these DESs and corresponding nanoemulsions were found to have fungicidal activities against *A. fumigatus*, *C. albicans*, *C. krusei*, and *T. mentagrophytes* strains. On one hand, DES C-in-water nanoemulsions exhibited a stronger bactericidal and fungicidal effect and on the other, they also required much lower amounts of individual components to display the same activity. For the investigation of the structure of the DESs and the DES-in-water emulsions, advanced NMR techniques were used.  $^1\text{H}$  NMR and  $^{13}\text{C}$  NMR signals confirmed the successful formation of DES through hydrogen bonding. Also, 2D NOESY and ROESY

experiments suggested that in the case of DES C-in-water emulsions, thymol remained in the core of the emulsion, suggesting that the hydrophilic end of raspberry ketone promoted the attachment of the DES (the functional component in the emulsions) on the cell membranes of the microbes. Thereafter, thymol may permeate through the cytoplasmic membrane altering its integrity. This explains the enhanced antimicrobial activity that was witnessed in the case of therapeutic DES and the DES-in-water nanoemulsions.

Therefore, the novelty of this work encompasses both formulation and characterization of novel natural compounds based DESs. These DESs and their corresponding DES-in-water nanoemulsions, formulated by sustainable membrane-based technologies, exhibited fungicidal properties against the aforementioned fungal strains. Also, scientific

cognizance of the observed antimicrobial effects was realized through advanced 1D and 2D NMR techniques in this work.

### CRedit authorship contribution statement

**S. Mondal:** Data curation, Formal analysis, Investigation, Methodology, Validation, Writing – original draft, Writing – review & editing, Visualization. **U.T. Syed:** Conceptualization, Data curation, Formal analysis, Investigation, Methodology, Validation, Visualization, Writing – original draft, Writing – review & editing, Supervision. **E. Pinto:** Investigation, Methodology, Writing – review & editing. **I.C. Leonardo:** Investigation, Methodology. **P. Romero:** Formal analysis, Investigation, Methodology, Validation, Writing – review & editing, Resources. **F.B. Gaspar:** Methodology, Validation, Writing – review & editing. **M.T. Barreto Crespo:** Resources, Supervision, Validation. **V. Sebastian:** Investigation, Methodology, Resources, Writing – review & editing. **J.G. Crespo:** Funding acquisition, Resources, Supervision, Validation, Writing – review & editing. **C. Brazinha:** Conceptualization, Funding acquisition, Project administration, Resources, Supervision, Validation, Writing – review & editing, Visualization.

### Declaration of competing interest

The authors declare that they have no known competing financial interests or personal relationships that could have appeared to influence the work reported in this paper.

### Data availability

No data was used for the research described in the article.

### Acknowledgement

SM acknowledges financial support from Fundação para a Ciência e a Tecnologia (FCT), Portugal for PhD grant SFRH/BD/146967/2019.

This research was supported by the Associate Laboratory for Green Chemistry - LAQV which is financed by national funds from FCT/MCTES (UIDB/50006/2020 and UIDP/50006/2020).

EP acknowledges support from national funds through FCT (Foundation for Science and Technology) within the scope of Base Funding UIDB/04423/2020 and UIDP/04423/2020 (CIIMAR).

IL, FG, TC acknowledge funding from INTERFACE Programme, through the Innovation, Technology and Circular Economy Fund (FITEC), as well as iNOVA4Health [UIDB/04462/2020 and UIDP/04462/2020] and LS4FUTURE [LA/P/0087/2020] programs financially supported by FCT and the Ministério da Ciência, Tecnologia e Ensino Superior (MCTES).

PR acknowledges financial support Grant PID2021-126132NB-I00 by MCIN/AEI/10.13039/501100011033 and the NMR Service of CEQMA (CSIC-UZ).

VS acknowledges financial support Grant PID2021-127847OB-I00 and PDC2022-133866-I00 by MCIN/AEI, as well the ELECMI (LMA node) and NANBIOSIS ICTSs.

### Appendix A. Supplementary data

Supplementary data to this article can be found online at <https://doi.org/10.1016/j.jclepro.2024.141167>.

### References

- Awad, T.S., Asker, D., Romsted, L.S., 2018. Evidence of coexisting microemulsion droplets in oil-in-water emulsions revealed by 2D DOSY 1H NMR. *J. Colloid Interface Sci.* 514, 83–92. <https://doi.org/10.1016/j.jcis.2017.12.024>.
- Bergua, F., Castro, M., Muñoz-Embid, J., Lafuente, C., Artal, M., 2021. Hydrophobic eutectic solvents: thermophysical study and application in removal of

- pharmaceutical products from water. *Chem. Eng. J.* 411, 128472 <https://doi.org/10.1016/J.CEJ.2021.128472>.
- Busić, V., Roca, S., Vikić-Topić, D., Vrandečić, K., Čosić, J., Molnar, M., Gašo-Sokač, D., 2020. Eco-friendly quaternization of nicotinamide and 2-bromoacetophenones in deep eutectic solvents. Antifungal activity of the products. *Environ. Chem. Lett.* 18, 889–894. <https://doi.org/10.1007/s10311-020-00973-3>.
- Cama, J., Henney, A.M., Winterhalter, M., 2019. Breaching the barrier: quantifying antibiotic permeability across gram-negative bacterial membranes. *J. Mol. Biol.* 431, 3531–3546. <https://doi.org/10.1016/j.jmb.2019.03.031>.
- Cao, J., Su, E., 2021. Hydrophobic deep eutectic solvents: the new generation of green solvents for diversified and colorful applications in green chemistry. *J. Clean. Prod.* 314, 127965 <https://doi.org/10.1016/J.JCLEPRO.2021.127965>.
- Charcosset, C., Limayem, I., Fessi, H., 2004. The membrane emulsification process - a review. *J. Chem. Technol. Biotechnol.* 79, 209–218. <https://doi.org/10.1002/jctb.969>.
- Chuchareon, T., Sabliov, C.M., 2019. Comparative effects of curcumin when delivered in a nanoemulsion or nanoparticle form for food applications: study on stability and lipid oxidation inhibition. *LWT* 113, 108319. <https://doi.org/10.1016/j.lwt.2019.108319>.
- D. Ribeiro, B., Florindo, C., Iff, C., Coelho, L.A.Z., M. M. Marrucho, I., 2015. Menthol-based eutectic mixtures: hydrophobic low viscosity solvents. *ACS Sustain. Chem. Eng.* 3, 2469–2477. <https://doi.org/10.1021/acssuschemeng.5b00532>.
- Escobar, A., Pérez, M., Romanelli, G., Blustein, G., 2020. Thymol bioactivity: a review focusing on practical applications. *Arab. J. Chem.* 13, 9243–9269. <https://doi.org/10.1016/j.arabjc.2020.11.009>.
- Espino, M., Solari, M., Fernández, M. de los Á., Boiteux, J., Gómez, M.R., Silva, M.F., 2019. NADES-mediated folk plant extracts as novel antifungal agents against *Candida albicans*. *J. Pharm. Biomed. Anal.* 167, 15–20. <https://doi.org/10.1016/j.jpba.2019.01.026>.
- Fisher, L.R., Mitchell, E.E., Parker, N.S., 1985. Interfacial tensions of commercial vegetable oils with water. *J. Food Sci.* 50, 1201–1202. <https://doi.org/10.1111/j.1365-2621.1985.tb13052.x>.
- Gallucci, M.N., Oliva, M., Casero, C., Dambolena, J., Luna, A., Zygodlo, J., Demo, M., 2009. Antimicrobial combined action of terpenes against the food-borne microorganisms *Escherichia coli*, *Staphylococcus aureus* and *Bacillus cereus*. *Flavour Fragr J* 24, 348–354. <https://doi.org/10.1002/ffj.1948>.
- Gao, Z., Li, X., Shi, L., Yang, Y., 2019. Deep eutectic solvents-derived carbon dots for detection of mercury (II), photocatalytic antifungal activity and fluorescent labeling for *C. albicans*. *Spectrochim. Acta Mol. Biomol. Spectrosc.* 220, 117080 <https://doi.org/10.1016/j.saa.2019.04.072>.
- Giüll, C., Ferrando, M., Schroën, K., 2016. 17 - membranes for enhanced emulsification processes. In: Knoerzer, K., Juliano, P., Smithers, G. (Eds.), *Woodhead Publishing Series in Food Science, Technology and Nutrition*. Woodhead Publishing, pp. 429–453. <https://doi.org/10.1016/B978-0-08-100294-0.00017-1>.
- Gupta, A., 2020. Chapter 21 - nanoemulsions. In: Chung, E.J., Leon, L., Rinaldi, C. (Eds.), *Micro and Nano Technologies*. Elsevier, pp. 371–384. <https://doi.org/10.1016/B978-0-12-816662-8.00021-7>.
- Häkkinen, R., Alshammari, O., Timmermann, V., D'Agostino, C., Abbott, A., 2019. Nanoscale clustering of alcoholic solutes in deep eutectic solvents studied by nuclear magnetic resonance and dynamic light scattering. *ACS Sustain. Chem. Eng.* 7, 15086–15092. <https://doi.org/10.1021/acssuschemeng.9b03771>.
- Hamdy, S.M., El-Khayat, Z., Farrag, A.R., Sayed, O.N., El-Sayed, M.M., Massoud, D., 2022. Hepatoprotective effect of Raspberry ketone and white tea against acrylamide-induced toxicity in rats. *Drug Chem. Toxicol.* 45, 722–730. <https://doi.org/10.1080/01480545.2020.1772279>.
- Hansen, B.B., Spittle, S., Chen, B., Poe, D., Zhang, Y., Klein, J.M., Horton, A., Adhikari, L., Zelovich, T., Doherty, B.W., Gurkan, B., Maginn, E.J., Ragauskas, A., Dadmun, M., Zawodzinski, T.A., Baker, G.A., Tuckerman, M.E., Savinell, R.F., Sangoro, J.R., 2021. Deep eutectic solvents: a review of fundamentals and applications. *Chem Rev* 121, 1232–1285. <https://doi.org/10.1021/acs.chemrev.0c00385>.
- Hassan, M., Kjos, M., Nes, I.F., Diep, D.B., Lotfipour, F., 2012. Natural antimicrobial peptides from bacteria: characteristics and potential applications to fight against antibiotic resistance. *J. Appl. Microbiol.* 113, 723–736. <https://doi.org/10.1111/j.1365-2672.2012.05338.x>.
- He, Q., Zhang, L., Yang, Z., Ding, T., Ye, X., Liu, D., Guo, M., 2022. Antibacterial mechanisms of thyme essential oil nanoemulsions against *Escherichia coli* O157:H7 and *Staphylococcus aureus*: alterations in membrane compositions and characteristics. *Innovat. Food Sci. Emerg. Technol.* 75, 102902 <https://doi.org/10.1016/j.ifset.2021.102902>.
- Jin, Y., Jung, D., Li, K., Park, K., Ko, J., Yang, M., Lee, J., 2019. Application of deep eutectic solvents to prepare mixture extracts of three long-lived trees with maximized skin-related bioactivities. *Appl. Sci.* <https://doi.org/10.3390/app9132581>.
- Kowalczyk, A., Przychozna, M., Sopata, S., Bodalska, A., Fecka, I., 2020. Thymol and thyme essential oil—new insights into selected therapeutic applications. *Molecules*. <https://doi.org/10.3390/molecules25184125>.
- Larsson, D.G.J., Flach, C.F., 2022. Antibiotic resistance in the environment. *Nat. Rev. Microbiol.* 20, 257–269. <https://doi.org/10.1038/s41579-021-00649-x>.
- Lee, K.P., Mattia, D., 2013. Manufacturing of nanoemulsions using nanoporous anodized alumina membranes: experimental investigation and process modeling. *Ind. Eng. Chem. Res.* 52, 14866–14874. <https://doi.org/10.1021/ie401960n>.
- Makoš, P., Przyjazny, A., Boczkaj, G., 2018. Hydrophobic deep eutectic solvents as “green” extraction media for polycyclic aromatic hydrocarbons in aqueous samples. *J. Chromatogr. A* 1570, 28–37. <https://doi.org/10.1016/J.CHROMA.2018.07.070>.

- Marchel, M., Cieřliński, H., Boczkaj, G., 2022. Deep eutectic solvents microbial toxicity: current state of art and critical evaluation of testing methods. *J. Hazard Mater.* 425, 127963 <https://doi.org/10.1016/J.JHAZMAT.2021.127963>.
- Marchel, M., Rayaroth, M.P., Wang, C., Kong, L., Khan, J.A., Boczkaj, G., 2023. Hydrophobic (deep) eutectic solvents (HDESs) as extractants for removal of pollutants from water and wastewater – a review. *Chem. Eng. J.* 475, 144971 <https://doi.org/10.1016/J.CEJ.2023.144971>.
- Maria José, Vale-Silva, Cavaleiro, Carlos, Salgueiro, Lúcia, Pinto, Eugénia, L.A.G., 2010. Antifungal activity of the essential oil of thymus x viciosoi against Candida, cryptococcus, Aspergillus and dermatophyte species. *Planta Med.* 76, 882–888. <https://doi.org/10.1055/s-0029-1240799>.
- Mietheke, M., Pieroni, M., Weber, T., Brönstrup, M., Hamann, P., Halby, L., Arimondo, P.B., Glaser, P., Aigle, B., Bode, H.B., Moreira, R., Li, Y., Luzhetskyy, A., Medema, M.H., Pernodet, J.-L., Stadler, M., Tormo, J.R., Genilloud, O., Truman, A. W., Weissman, K.J., Takano, E., Sabatini, S., Stegmann, E., Brötz-Oesterhelt, H., Wohlleben, W., Seemann, M., Empting, M., Hirsch, A.K.H., Loretz, B., Lehr, C.-M., Titz, A., Herrmann, J., Jaeger, T., Alt, S., Hestekamp, T., Winterhalter, M., Schiefer, A., Pfarr, K., Hoerauf, A., Graz, H., Graz, M., Lindvall, M., Ramurthy, S., Karlén, A., van Dongen, M., Petkovic, H., Keller, A., Peyrane, F., Donadio, S., Fraisse, L., Piddock, L.J.V., Gilbert, I.H., Moser, H.E., Müller, R., 2021. Towards the sustainable discovery and development of new antibiotics. *Nat. Rev. Chem.* 5, 726–749. <https://doi.org/10.1038/s41570-021-00313-1>.
- Momotko, M., Łuczak, J., Przyjazny, A., Boczkaj, G., 2022. A natural deep eutectic solvent - protonated L-proline-xylitol - based stationary phase for gas chromatography. *J. Chromatogr. A* 1676, 463238. <https://doi.org/10.1016/J.CHROMA.2022.463238>.
- Mondal, S., Alke, B., de Castro, A.M., Ortiz-Albo, P., Syed, U.T., Crespo, J.G., Brazinha, C., 2022. Design of enzyme loaded W/O emulsions by direct membrane emulsification for CO<sub>2</sub> capture. *Membranes*. <https://doi.org/10.3390/membranes12080797>.
- Mondal, S., Syed, U.T., Gil, C., Hilliou, L., Duque, A.F., Reis, M.A.M., Brazinha, C., 2023. A novel sustainable PHA downstream method. *Green Chem.* 25, 1137–1149. <https://doi.org/10.1039/D2GC004261D>.
- PA, W., 2002. Reference method for broth dilution antifungal susceptibility testing of yeasts. Approved Standard-CLSI document M27-A2, 22 (15).
- PA, W., 2008. Clinical and Laboratory Standards Institute (Clis): Reference Method for Broth Dilution Antifungal Susceptibility Testing of Filamentous Fungi. Approved Standard-CLSI document M38-A2.
- PA, W., 2015. In: Methods for Dilution Antimicrobial Susceptibility Tests for Bacteria that Grow Aerobically—Tenth Edition. Approved Standard-CLSI document M07-A10.
- Peña-Gómez, N., Ruiz-Rico, M., Pérez-Esteve, É., Fernández-Segovia, I., Barat, J.M., 2019. Novel antimicrobial filtering materials based on carvacrol, eugenol, thymol and vanillin immobilized on silica microparticles for water treatment. *Innovat. Food Sci. Emerg. Technol.* 58, 102228 <https://doi.org/10.1016/j.ifset.2019.102228>.
- Piacentini, E., Drioli, E., Giorno, L., 2014a. Membrane emulsification technology: twenty-five years of inventions and research through patent survey. *J. Membr. Sci.* 468, 410–422. <https://doi.org/10.1016/J.MEMSCI.2014.05.059>.
- Piacentini, E., Drioli, E., Giorno, L., 2014b. Pulsed back-and-forward cross-flow batch membrane emulsification with high productivity to obtain highly uniform and concentrate emulsions. *J. Membr. Sci.* 453, 119–125. <https://doi.org/10.1016/j.memsci.2013.10.063>.
- Prakash, A., Baskaran, R., Paramasivam, N., Vadivel, V., 2018. Essential oil based nanoemulsions to improve the microbial quality of minimally processed fruits and vegetables: a review. *Food Res. Int.* 111, 509–523. <https://doi.org/10.1016/j.foodres.2018.05.066>.
- Rodríguez-Juan, E., López, S., Abia, R., J. G. Muriana, F., Fernández-Bolaños, J., García-Borrego, A., 2021. Antimicrobial activity on phytopathogenic bacteria and yeast, cytotoxicity and solubilizing capacity of deep eutectic solvents. *J. Mol. Liq.* 337, 116343 <https://doi.org/10.1016/J.MOLLIQ.2021.116343>.
- Schultheiss, N., Newman, A., 2009. Pharmaceutical cocrystals and their physicochemical properties. *Cryst. Growth Des.* 9, 2950–2967. <https://doi.org/10.1021/cg900129f>.
- Shu, M., Zhu, L., Yuan, M., Wang, L., Wang, Y., Yang, L., Sha, Z., Zeng, M., 2017. Solubility and solution thermodynamic properties of 4-(4-Hydroxyphenyl)-2-butanone (raspberry ketone) in different pure solvents. *J. Solut. Chem.* 46, 1995–2013. <https://doi.org/10.1007/s10953-017-0681-0>.
- Silva, J.M., Silva, E., Reis, R.L., Duarte, A.R.C., 2019. A closer look in the antimicrobial properties of deep eutectic solvents based on fatty acids. *Sustain. Chem. Pharm.* 14, 100192 <https://doi.org/10.1016/j.scp.2019.100192>.
- Silva, E., Oliveira, F., Silva, J.M., Reis, R.L., Duarte, A.R.C., 2021. Untangling the bioactive properties of therapeutic deep eutectic solvents based on natural terpenes. *Current Res. Chem. Biol.* 1, 100003 <https://doi.org/10.1016/j.crchbi.2021.100003>.
- Smith, E.L., Abbott, A.P., Ryder, K.S., 2014. Deep eutectic solvents (DESs) and their applications. *Chem. Rev.* 114, 11060–11082. <https://doi.org/10.1021/cr300162p>.
- Syed, U.T., Leonardo, I., Lahoz, R., Gaspar, F.B., Huertas, R., Crespo, M.T.B., Arruebo, M., Crespo, J.G., Sebastian, V., Brazinha, C., 2020. Microengineered membranes for sustainable production of hydrophobic deep eutectic solvent-based nanoemulsions by membrane emulsification for enhanced antimicrobial activity. *ACS Sustain. Chem. Eng.* 8, 16526–16536. <https://doi.org/10.1021/acssuschemeng.0c05612>.
- Syed, U.T., Dias, A.M.A., Crespo, J., Brazinha, C., de Sousa, H.C., 2021. Studies on the formation and stability of perfluorodecalin nanoemulsions by ultrasound emulsification using novel surfactant systems. *Colloids Surf. A Physicochem. Eng. Asp.* 616, 126315 <https://doi.org/10.1016/j.colsurfa.2021.126315>.
- Syed, U.T., Usman, Dias, A.M.A., de Sousa, H.C., Crespo, J., Brazinha, C., 2022. Greening perfluorocarbon based nanoemulsions by direct membrane emulsification: comparative studies with ultrasound emulsification. *J. Clean. Prod.* 357, 131966 <https://doi.org/10.1016/j.jclepro.2022.131966>.
- Syed, Usman T., Leonardo, I.C., Mendoza, G., Gaspar, F.B., Gámez, E., Huertas, R.M., Crespo, M.T.B., Arruebo, M., Crespo, J.G., Sebastian, V., Brazinha, C., 2022. On the role of components of therapeutic hydrophobic deep eutectic solvent-based nanoemulsions sustainably produced by membrane-assisted nanoemulsification for enhanced antimicrobial activity. *Sep. Purif. Technol.* 285, 120319 <https://doi.org/10.1016/j.seppur.2021.120319>.
- van Osch, D.J.G.P., Zubeir, L.F., van den Bruinhorst, A., Rocha, M.A.A., Kroon, M.C., 2015. Hydrophobic deep eutectic solvents as water-immiscible extractants. *Green Chem.* 17, 4518–4521. <https://doi.org/10.1039/C5GC01451D>.
- Van Osch, D.J.G.P., Dietz, C.H.J.T., Warrag, S.E.E., Kroon, M.C., 2020. The curious case of hydrophobic deep eutectic solvents: a story on the discovery, Design, and applications. *ACS Sustain. Chem. Eng.* 8, 10591–10612. <https://doi.org/10.1021/acssuschemeng.0c00559>.
- Yue, Y., Gong, X., Jiao, W., Li, Y., Yin, X., Si, Y., Yu, J., Ding, B., 2021. In-situ electrospinning of thymol-loaded polyurethane fibrous membranes for waterproof, breathable, and antibacterial wound dressing application. *J. Colloid Interface Sci.* 592, 310–318. <https://doi.org/10.1016/j.jcis.2021.02.048>.
- Zeng, C., Liu, Y., Ding, Z., Xia, H., Guo, S., 2021. Physicochemical properties and antibacterial activity of hydrophobic deep eutectic solvent-in-water nanoemulsion. *J. Mol. Liq.* 338, 116950 <https://doi.org/10.1016/j.molliq.2021.116950>.
- Zhang, Y., Qiao, Q., Abbas, U.L., Liu, J., Zheng, Y., Jones, C., Shao, Q., Shi, J., 2023. Lignin derived hydrophobic deep eutectic solvents as sustainable extractants. *J. Clean. Prod.* 388, 135808 <https://doi.org/10.1016/J.JCLEPRO.2022.135808>.